ELSEVIER

International Journal of Mass Spectrometry and Ion Processes 163 (1997) 131–139

International Journal of Mass Spectrometry and Ion Processes

Electron-impact ionization of nitric acid

Caroline S.S. O'Connor, Nykola C. Jones, Stephen D. Price*

Chemistry Department, University College London, Christopher Ingold Laboratories, 20 Gordon Street, London WC1H 0AJ, UK

Received 4 November 1996; accepted 2 December 1996

Abstract

Relative partial ionization cross sections of nitric acid have been determined for incident electron energies from 40 to 450 eV using time-of-flight mass spectrometry. The experiments detect stable parent ions, HNO_3^+, and the fragmentation products H^+, N^+, O^+, OH^+, NO^+ and NO_2^+. The ionic decay channel involving the formation of H^+ has been observed for the first time and the appearance energy of this fragment has been determined to lie between 55 and 60 eV. © 1997 Elsevier Science B.V.

Keywords: Electron ionization; Nitric acid; Relative partial ionization cross section; Time-of-flight mass spectrometry

1. Introduction

Nitric acid, HNO_3, is an important trace constituent in the Earth's upper atmosphere and plays a key role in the complex chemistry of the stratospheric ozone cycle. Nitric acid is a reservoir molecule for nitrogen oxides, NO_x, which are involved in the generation and destruction of ozone and other significant atmospheric effects [1]. In the lower stratosphere NO_x radicals are generated by the photolysis of nitric acid, while the main depletion process for stratospheric NO_x involves the formation of nitric acid which is subsequently rained out of the atmosphere.

Despite the atmospheric significance of nitric acid there have been few investigations of its ionization. In fact the mass spectrum of nitric acid has not been well characterised and is not reported in either the Eight Peak Index of Mass Spectra [2] or the NIST database. The two studies of the ionization of nitric acid reported in the literature are an early electron-impact study at an unspecified electron energy [3] and a more recent photoionization study employing photons with energies between 10 and 20 eV [4].

As part of an ongoing investigation of the ionization of reactive species, this paper presents a determination of the relative partial ionization cross sections of HNO_3 over a range of electron energies from 45 to 450 eV using time-of-flight mass spectrometry. We also report the appearance energy of previously unobserved fragmentation of HNO_3^+ to form H^+. Quantitative studies of molecular ionization such as this, provide experimental data for comparison with theoretical models of electron/molecule scattering [5–7]. They also lead us towards a detailed understanding of the properties of molecular ions, such as HNO_3^+, allowing the modeling of their role in energized media such as plasmas and interstellar environments.

* Corresponding author

0168-1176/97/$17.00 © 1997 Elsevier Science B.V. All rights reserved
PII S0168-1176(96)04536-3

The lack of available data concerning the mass spectrum of HNO_3 and its ionization is undoubtedly due to the inherent difficulty in preparing a pure sample of this very reactive molecule, which makes the recording of reproducible mass spectra problematic. The reactive nature of nitric acid presents further problems as it has a tendency to decompose on contact with the many metallic and non-metallic surfaces commonly found in the inlet systems of mass spectrometers [8]. Therefore, considerable care must be taken to prepare a pure sample of nitric acid and allow it to reach the ionization region of the mass spectrometer rapidly, without any decomposition. As described below, these problems were overcome in this work by careful sample preparation and the use of a clean, non-catalytic inlet system for the time-of-flight mass spectrometer.

2. Experimental

The relative partial ionization cross sections of nitric acid were derived from mass spectra recorded at a range of energies from 40 to 450 eV using a time-of-flight mass spectrometer of the standard Wiley–McLaren design [9]. This apparatus is illustrated schematically in Fig. 1 and its detailed description has been presented in a previous publication [8]. In brief, ionization events occur at the centre of the source region of the time-of-flight mass spectrometer, at the intersection of an effusive jet of the target gas with an electron beam. The target gas and the electron beam are transported into the centre of the source region via hypodermic needles. These two hypodermic needles are orientated orthogonal to one another and to the axis of the time-of-flight mass spectrometer. The ends of both needles are situated approximately 2 mm from the axis of the time-of-flight mass spectrometer. The intensity of the electron beam is stabilised so that an electron current of less than 0.5 nA passes down the needle (Fig. 1) and crosses the interaction region. The energy of the electron beam was calibrated by the determination of the ionization thresholds of argon, and in these experiments a conservative estimate of the uncertainty in the electron energy was found to be ± 2 eV.

To record a time-of-flight mass spectrum, the repeller plate (Fig. 1) is pulsed to + 200 V and ions present in the source region are accelerated towards the channeltron detector. The subsequent arrival times of the positive ions at the detector are recorded using a multichannel scalar (EG&G Turbo-MCS). An extraction pulse width of 20 μs

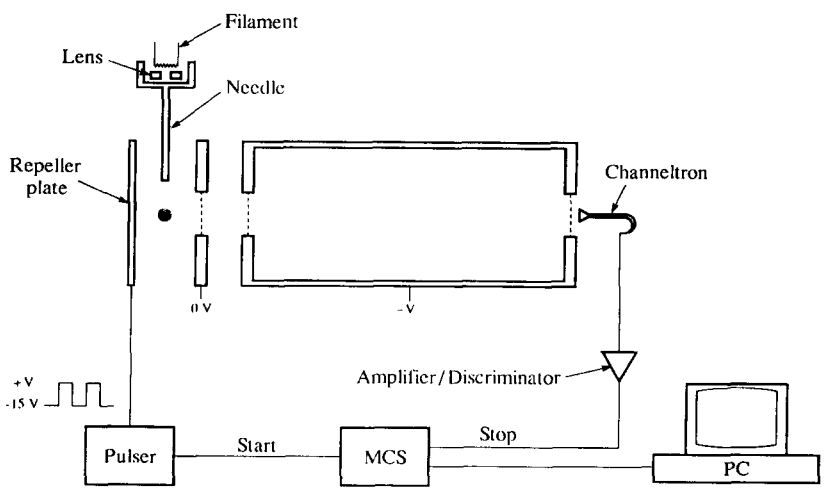

Fig. 1. Schematic diagram of the time-of-flight mass spectrometer. The gas inlet is perpendicular to the plane of the figure and is not shown.

was employed with a period of 50 μs. As has been discussed before [10], problems can be encountered with this experimental arrangement due to the trapping of ions which have low translational energies within the space-charge of the electron beam. Such trapping could lead to discrimination effects in the mass spectra [10,11]. To overcome this electrostatic attraction of the electron beam, a negative bias voltage (15–20 V) is applied to the repeller plate during the interpulse period. As a result, any ions formed during this period are accelerated out of the interaction region, and the potential well of the electron beam, towards the repeller plate. An indication that the application of this bias voltage eliminates any trapping effects is that the relative intensities of the ion signals in the mass spectra are now seen to be insensitive to variations in the electron beam current, and the duration, width and duty cycle of the extraction pulse [8].

As described above, the presence of the bias field results in the ions formed during the interpulse period being immediately accelerated towards the repeller plate. Therefore, ions of different masses formed with the same partial ionization cross section will have different densities in the source region, due to their differing velocities across it. A correction factor must therefore be applied to the intensity ratio from the mass spectra to yield the ratio of the partial ionization cross sections [8]. The calculation of this correction factor is discussed below. Using such a correction factor, the mass spectra of argon from our apparatus yield a ratio of single to double ionization cross sections in good agreement with that available in the literature [11].

The nitric acid sample used for these experiments was prepared by dehydration of a commercially purchased sample of nitric acid (HNO_3 content $> 90\%$) by repeated vacuum distillation over P_2O_5. During the mass spectrometric experiments the anhydrous liquid acid was kept in a salted ice bath, at a temperature of approximately 255 K. To avoid degradation of the HNO_3 molecules before they reach the ionization region of the mass spectrometer, a wide bore, high conductance inlet system was used to draw rapidly the HNO_3 molecules which vaporize from the sample into the mass spectrometer. The inlet system is constructed of glass and Teflon to ensure it is clean and non-catalytic. Indeed, the only metallic part of the inlet system is the hypodermic needle which transports the gaseous HNO_3 into the source region. The amount of gaseous HNO_3 flowing into the mass spectrometer was controlled by slight variations in the temperature of the ice bath.

Typical operating pressures in the mass spectrometer, as recorded by an ion gauge, were of the order of 6×10^{-5} Pa. As discussed previously [10], low operating pressures in the time-of-flight mass spectrometer are required to avoid channeltron saturation, which leads to reduced detection efficiency and biased ion intensities. The low operating pressures, in conjunction with the selection of the optimal emission current for each electron energy, maintained an average ion count rate of approximately 0.1 ions per pulse, which eliminates the effects of channeltron saturation.

3. Data analysis

A typical mass spectrum for HNO_3 is shown in Fig. 2. As can be seen from this figure, the stable parent ion (HNO_3^+) and fragment ions H^+, N^+, O^+, OH^+, NO^+ and NO_2^+ are detected. The spectra also contain small signals resulting from traces of air in the sample and water, the principal background gas in the apparatus.

The mass spectra (Fig. 2) have a "stepped" background which is due to the formation of ions during the + 200 V extraction pulse [8]. As mentioned above, the application of the extraction pulse accelerates ions towards the detector, but it also deflects the electron beam so that ionization no longer occurs in the focused volume. Some of the ions formed by the deflected electron beam do, however, reach the detector, although

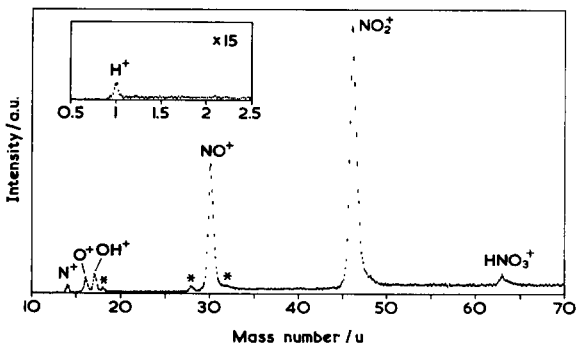

Fig. 2. A typical time-of-flight mass spectrum of HNO_3 at an electron energy of 150 eV. The error bars shown are of length 2σ, where σ is derived from the counting statistics. The peaks marked with asterisks correspond to signals (H_2O^+, N_2^+ and O_2^+) due to traces of air and water from the residual gas.

they arrive later than ions of the same mass that were in the focused volume when the extraction pulse was applied. These longer flight times, which are due to the formation of the background ions after the application of the extraction pulse and to their formation away from the centre of the source, result in a stepped background.

The raw data obtained from the mass spectra consist of the intensities of the ion signals recorded at a range of electron energies from 40 to 450 eV. The intensities of the ion signals are determined by finding the area of the peaks and applying a suitable background correction. The ion signal intensities are related to the partial ionization cross sections as described below. To remove any contribution from the ionization of the traces of air and water in the source region to the H^+, N^+, O^+, OH^+ and O_2^+ signals in the nitric acid spectrum, we recorded mass spectra of air and water over the range of electron energies employed in the experiments. From these spectra we determined the relative intensities of the H^+, N^+, O^+, OH^+ and O_2^+ ions with respect to N_2^+ for the air spectra and H_2O^+ for the water spectra. The contribution of the ionization of air or water to the H^+, N^+, O^+, OH^+ and O_2^+ signals in the nitric acid spectra can then be accurately determined, and subtracted, by scaling the relative intensities of the fragment ions from the air and water spectra using the N_2^+ and H_2O^+ signals in the nitric acid spectra, as the N_2^+ and H_2O^+ signals in the nitric acid spectra can only arise from background gas. This background correction is found to be negligible for the H^+ and O^+ fragment ion signals but accounts for all the O_2^+ ion signal in the nitric acid spectrum, within the experimental uncertainty. To determine the partial ionization cross sections, the intensities of the H^+, N^+, O^+, OH^+, NO^+ and HNO_3^+ ion signals are divided by the intensity of the peak of the most abundant fragment, NO_2^+, to give an intensity ratio, $I_{X^+}/I_{NO_2^+}$, for each fragment. However, due to the ion density effects described above, a correction factor must be applied to this intensity ratio to give the relative partial ionization cross section, $\sigma_{X^+}/\sigma_{NO_2^+}$. As has been shown before [8], ions formed at the same rate in the source will have a density ratio equal to the ratio of the square root of their masses and so an appropriate mass factor (Eq. (1)) is applied to the intensity ratio to give the relative partial ionization cross section. For example, for a fragment ion X^+

$$\frac{\sigma_{X^+}}{\sigma_{NO_2^+}} = \frac{\sqrt{m_{NO_2^+}}}{\sqrt{m_{X^+}}} \frac{I_{X^+}}{I_{NO_2^+}} \quad (1)$$

where m is the relative molecular mass of the ion.

Due to the small collection aperture of the channeltron detector, ions formed with a translational energy of more than 0.3 eV perpendicular to the axis of the spectrometer will miss the detector. Therefore the analysis procedure applied above to the fragment ion signals is valid only if an insignificant proportion of fragment ions is produced with kinetic energies above 0.3 eV [8]. Investigations into the fragmentation of triatomic ions formed by electron-impact [8,12] indicate that only a small percentage of the fragment ions from these species have kinetic energies greater than 0.3 eV. Due to the increased number of available internal modes, one would expect a similar, if not smaller, proportion of high kinetic energy fragments to result from the dissociation of the polyatomic HNO_3^+ ion. Therefore it can be concluded that the analysis procedure described

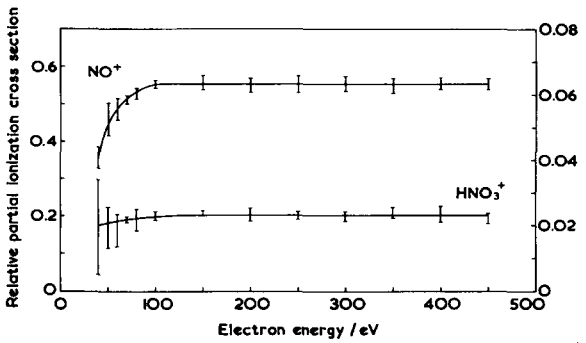

Fig. 3. Relative partial ionization cross sections for forming NO^+ and HNO_3^+ from nitric acid, relative to the most abundant ion in the mass spectrum, NO_2^+. See text for details. The values for HNO_3^+ should be read from the right-hand axis. The error bars represent two standard deviations. The solid lines drawn through the points are to guide the eye.

above yields accurate values of partial ionization cross sections, a conclusion supported by previous work [8,10].

The geometric constraints of the channeltron aperture described above discriminate strongly against the energetic fragments produced by the dissociation of multiply charged ions. Thus, if fragment ions are formed by both single ionization and double ionization, the relative partial ionization cross section we measure is dominated by single ionization [13] and could be correctly termed a partial single ionization cross section.

Relative partial ionization cross sections for HNO_3 derived by the analysis procedure described above, at incident electron energies

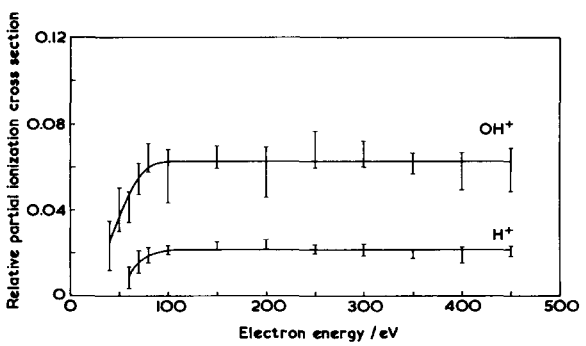

Fig. 4. Relative partial ionization cross sections for forming OH^+ and H^+ from nitric acid, relative to NO_2^+. See Fig. 3 caption for details.

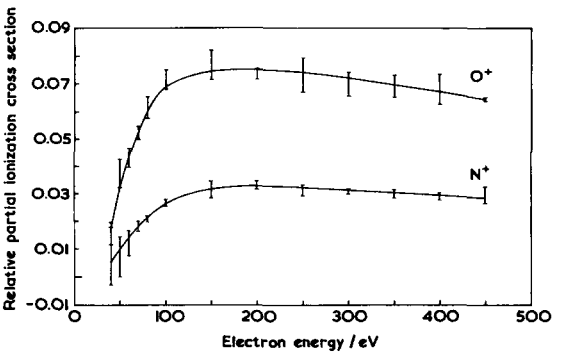

Fig. 5. Relative partial ionization cross sections for forming O^+ and N^+ from nitric acid, relative to NO_2^+. See Fig. 3 caption for details.

from 40 to 450 eV, are shown in Figs. 3–5 and listed in Table 1. These values are the average of six independent determinations. The standard deviation of these determinations at each electron energy is also shown in Table 1 and plotted as the error bars in Figs. 3–5. The standard deviations are small, better than 8% at points away from the lowest electron energies, in accord with the small statistical (counting) error in each individual determination. Note that the density correction for the light H^+ fragments involves scaling by a large factor (Eq. (1)), therefore amplifying any errors inherent in the analysis procedure. The standard deviations in the relative partial ionization cross sections do not, however, take into account any systematic errors present in the experiment due to, for example, any unresolved mass-dependent detection efficiencies. But, due to the efforts described above to resolve any such problems and the good agreement between previous partial ionization cross sections derived using this apparatus and literature values [8,10], the standard deviations quoted are considered to provide a good estimate of the error in the reported values.

In the two previous investigations of the ionization and fragmentation of nitric acid reported in the literature [3,4], no H^+ fragment ions were detected. The detection of H^+ fragments in the current work is undoubtedly due to the higher ionizing energies employed and the absence of

Table 1
Relative partial ionization cross sections for the formation of the indicated product ion from HNO_3 (the numbers in parentheses indicate the standard deviation in the last figure of each cross section)

Electron energy/eV	Relative partial ionization cross section $\sigma_{X^+}/\sigma_{NO_2^+}$					
	H^+	N^+	O^+	OH^+	NO^+	HNO_3^+
40		0.007(10)	0.0154(40)	0.024(12)	0.356(29)	0.0195(145)
50		0.0070(72)	0.0374(52)	0.040(10)	0.459(44)	0.0192(62)
60	0.0085(50)	0.0119(45)	0.0430(35)	0.0415(71)	0.486(29)	0.0184(50)
70	0.0159(52)	0.0181(19)	0.0523(23)	0.0546(73)	0.511(11)	0.0217(9)
80	0.0190(37)	0.0207(12)	0.0614(39)	0.0644(66)	0.527(15)	0.0215(33)
100	0.0213(21)	0.0265(13)	0.0714(35)	0.056(13)	0.552(11)	0.0228(14)
150	0.0232(19)	0.0314(31)	0.0767(53)	0.0645(54)	0.557(19)	0.0236(8)
200	0.0240(22)	0.0330(15)	0.0735(20)	0.058(12)	0.550(19)	0.0232(20)
250	0.0216(21)	0.0312(20)	0.0732(62)	0.0681(87)	0.552(23)	0.0229(12)
300	0.0212(27)	0.0307(10)	0.0698(43)	0.0659(61)	0.554(20)	0.0227(16)
350	0.0191(19)	0.0299(15)	0.0691(40)	0.0615(49)	0.549(20)	0.0239(17)
400	0.0188(37)	0.0288(13)	0.0680(55)	0.0579(87)	0.555(16)	0.0234(24)
450	0.0206(25)	0.0294(31)	0.0644(7)	0.059(10)	0.553(15)	0.0220(16)

any discrimination against light ions such as may be present in the quadrupole mass spectrometer used in the photoionization study [4]. In order to determine the appearance energy of this newly observed fragment, the relative partial ionization cross sections for the formation of H^+ from HNO_3^+ were evaluated at electron energies from 45 to 80 eV and are given in Table 2. These values are the average of three independent determinations and the standard deviations of these determinations at each electron energy are also shown in Table 2. By inspection, the appearance energy for the H^+ fragment is determined to lie between 55 and 60 eV. A more accurate determination of this appearance energy is very difficult as the statistical (counting) uncertainties in the weak H^+ signal are large near threshold. The appearance energies for the fragment ions OH^+, NO^+ and NO_2^+ have been previously determined at better energy resolution [4] than can be achieved using the current experimental arrangement and were therefore not redetermined in this study.

Table 2
Relative partial ionization cross section for the formation of H^+ from HNO_3 at low ionizing electron energies. The standard deviation in the last figure of each cross section is given in parentheses. By inspection, the appearance energy for H^+ is determined to lie between 55 and 60 eV

Electron energy/eV	$\sigma_{H^+}/\sigma_{NO_2^+}$
45	−0.030(25)
50	0.005(18)
55	−0.007(12)
60	0.0089(60)
65	0.0153(51)
70	0.0207(44)
75	0.0159(42)
80	0.0292(36)

4. Discussion

As mentioned above, there have only been two previous reports in the literature concerning the ionization and fragmentation of HNO_3, one study using photoionization mass spectrometry (PIMS) in the energy range 10–20 eV [4], and a second early study employing electron-impact ionization mass spectrometry (EIMS) [3] at an unspecified ionizing energy. In the electron-impact study [3] NO_2^+, NO^+, O_2^+, OH^+, O^+ and N^+ fragment ions were observed, in addition to the parent ion HNO_3^+ and significant impurity peaks. The NO_2^+ signal was observed to be more abundant than the NO^+ signal. In the photoionization work [4], NO_2^+, NO^+, O_2^+, OH^+, O^+ and N^+ fragment ions were again observed but no parent ions were

detected and, in contrast to the EIMS work, NO^+ ions were more abundant than NO_2^+. In addition, this photoionization study determined the appearance energies of the NO_2^+, NO^+ and OH^+ fragment ions to be 11.90 eV, 13.07 eV and 16.60 eV respectively [4].

In the present study, at electron energies from 40 to 450 eV, the parent ion HNO_3^+ and fragment ions NO_2^+, NO^+, OH^+, O^+, N^+ and H^+ were detected. The most abundant fragment was found to be NO_2^+ (Fig. 2). The plots of the relative partial ionization cross sections of the ions against electron energy (Figs. 3–5) all show an initial increase in the relative partial ionization cross section as the electron energy is raised. This increase is due to the fact that ionic fragmentation becomes more likely with increasing electron energy and associated ionic excitation. In both the EIMS and PIMS experiments [3,4], O_2^+ fragment ions were detected, but at very low intensities. In this study, once the contribution from the small amount of residual gas has been subtracted, the relative partial ionization cross section for the formation of O_2^+ from HNO_3^+, within our error limits, is zero.

In the current work, the intensity ratio of NO_2^+ to NO^+ at the lowest energy (40 eV) is approximately 3:1 (Fig. 3, Table 1). The EIMS study also found the NO_2^+ ion to be more abundant than the NO^+ ion, although the ratio was found to be only 6:5 [3]. However, the electron energy used in the EIMS work is unspecified and no valid comparison can really be made. The intensity ratio of NO_2^+ to NO^+ in the present work is, however, significantly different to that presented in the PIMS study using 20.7 eV photons [4], where the NO^+ signal was observed to be larger than the NO_2^+ signal. The presence of the hot filament in our electron-impact mass spectrometer could stimulate the thermal decomposition of the HNO_3 to form NO_2 resulting in an increased NO_2^+ signal. However, an earlier study of the dissociation and fragmentation of $N_2O_5^+$ using the current experimental arrangement [10], where any apparatus-induced thermal decomposition should have been apparent, yielded an NO_2^+ to NO^+ ratio in good accord with previous photoionization work [4]. Therefore, we do not consider the larger yield of NO_2^+ in the current experiments to be due to thermal effects.

In the earlier EIMS study [3], the parent ion HNO_3^+ was observed in the mass spectrum. Such signals were also observed in the current work. These observations are contrary to the results of the PIMS study where no parent ions were detected [4]. There are a number of possible explanations for this fundamental difference between the mass spectra obtained using electron-impact ionization and those obtained using photoionization. One such explanation is that there is a bound state of HNO_3^+ lying above the energy of the ionizing photons used in the PIMS work (20.7 eV). This is however unlikely, as such a state would lie above the majority of the dissociation asymptotes of HNO_3^+ and would thus be expected to predissociate rapidly. Alternatively, in the electron-impact experiments there could be a resonant attachment process occurring, with rapid subsequent autodetachment to form the parent monocation (Eq. (2))

$$e^- + HNO_3 \rightarrow HNO_3^{*-} \rightarrow HNO_3^+ + 2e^- \qquad (2)$$

The autodetachment process could populate bound regions of the HNO_3 potential energy surface which are not accessible in direct ionization. This attachment process is, however, unlikely to occur at the high electron energies used in the current experiments.

A further possible explanation for the HNO_3^+ signal is the differing experimental arrangements used in electron-impact and photoionization mass spectrometry. Unusual ions can be observed in electron-impact mass spectra due to dissociation processes occurring at the hot filament and subsequent chemical reactions. It is easy to imagine how this process could result in unusual "fragment" molecules which are subsequently ionized, but more difficult to see how it could lead to HNO_3 molecules in states not populated in the nascent HNO_3 sample, which could then be

ionized to a bound region of the HNO_3^+ potential energy surface.

Perhaps the most probable explanation for the discrepancy between the parent ion signals observed when employing the different forms of ionization is that, following electron-impact, the nitric acid molecule is promoted into an excited state which subsequently autoionizes to form the parent monocation (Eq. (3))

$$HNO_3 + e^- \rightarrow HNO_3^* + e^- \rightarrow HNO_3^+ + 2e^- \quad (3)$$

The excited state of the neutral molecule, which subsequently autoionizes to form the stable HNO_3^+ ion, could either lie above the energy of the photons used in the PIMS work, or is formed as a result of a transition which cannot be accessed by photoionization.

As described above, the appearance energy for the formation of H^+ from HNO_3^+ has been determined to lie between 55 and 60 eV. The thermodynamic asymptotes of the various monocation fragmentation reactions to form H^+, together with other neutral species, lie well below the determined appearance energy for this fragment. For example, the most energetically demanding dissociation pathway involves the complete fragmentation of the HNO_3^+ ion (Eq. (4)), and has a thermodynamic asymptote of 29.9 eV [14], assuming all the fragments are formed in their ground states

$$HNO_3^+ \rightarrow H^+ + N + 3O \quad (4)$$

This thermodynamic asymptote is significantly lower than our determination of the H^+ appearance energy, which leads us to consider that the formation of H^+ ions is most probably due to the double ionization of nitric acid. The double ionization energy of nitric acid can be estimated as 33.46 eV by the "rule of thumb" [15], and it is satisfying to note that the determined appearance energy for the H^+ fragment lies above this double ionization energy. Current studies of the formation and fragmentation of the HNO_3 dication, using ion–ion coincidence techniques [16], indicate that a large number of H^+ ions are produced upon dissociation of HNO_3^{2+}. For example, one such dissociation pathway is shown in Eq. (5)

$$HNO_3^{2+} \rightarrow H^+ + NO_2^+ + O \quad (5)$$

Due to the geometric discrimination effects described above, it would be expected that any fragments formed by double ionization are detected very inefficiency by our apparatus, due to their significant kinetic energies. However, if the formation of H^+ from HNO_3^{2+} has a significant probability, then the small number of H^+ ions which receive impulses along the axis of the spectrometer will be detected in the time-of-flight mass spectrum. If dicationic charge separation is indeed the principal source of H^+ ions, the markedly lower detection efficiency for these energetic species will mean that our measured partial ionization cross sections should be considered as a lower limit.

The results presented in this study show that there are major discrepancies between the ion yields of the ionization and fragmentation of nitric acid using photoionization and electron-impact mass spectrometry. These differences include the observation of stable parent HNO_3^+ ions in the electron-impact mass spectra, but not in the photoionization mass spectra, and markedly differing abundances of NO^+ and NO_2^+ fragment ions. The ionization of nitric acid obviously requires further investigation to determine whether these discrepancies are a result of fundamental differences between photons and electrons as ionizing agents, or more subtle experimental factors.

5. Conclusion

This study presents a determination of relative partial ionization cross sections of nitric acid for incident electron energies from 40 to 450 eV using time-of-flight mass spectrometry. Stable parent ions HNO_3^+ and H^+, N^+, O^+, OH^+, NO^+ and NO_2^+ fragment ions were detected, the most abundant ion being NO_2^+. The appearance energy

for the previously unobserved H^+ fragment was determined to lie between 55 and 60 eV, and its formation is considered to be due to the dissociation of the nitric acid dication, HNO_3^{2+}.

Acknowledgements

We would like to thank UCL and the Nuffield Foundation for financial support, the Central Research Fund of the University of London for an equipment grant and the EPSRC for the award of a research studentship for C.S.S.O'C.

References

[1] B.A. Thrush, Rep. Prog. Phys. 51 (1988) 1341.
[2] Eight Peak Index of Mass Spectra, Vol. 1, Mass Spectra Data Centre, 1970.
[3] R.A. Friedel, J.L. Shultz, A.G. Sharkey, Anal. Chem. 31 (1959) 1128.
[4] H.-W. Jochims, W. Denzer, H. Baumgärtel, O. Lösking, H. Willner, Ber. Bunsenges. Phys. Chem. 96 (1992) 573.
[5] K.N. Joshipura, Indian J. Pure Appl. Phys. 23 (1985) 525.
[6] K.N. Joshipura, Pramana 32 (1989) 139.
[7] Y. Okamoto, Y. Itikawa, Chem. Phys. Lett. 203 (1993) 61.
[8] K.A. Newson, S.M. Luc, S.D. Price, N.J. Mason, Int. J. Mass Spectrom. Ion. Proc. 148 (1995) 203.
[9] W.C. Wiley, I.H. McLaren, Rev. Sci. Instrum. 26 (1955) 1150.
[10] C.S.S. O'Connor, N.C. Jones, K. O'Neale, S.D. Price, Int. J. Mass Spectrom. Ion. Proc. 154 (1996) 203.
[11] M.R. Bruce, R.A. Bonham, Z. Phys. D 24 (1992) 149.
[12] R. Locht, G. Hagenow, K. Hottmann, H. Baumgärtel, Chem. Phys. 151 (1991) 137.
[13] T.D. Märk, in: T.D. Märk, G.H.Dunn (Eds.), Electron Impact Ionization, Springer-Verlag, New York, 1985.
[14] S.G. Lias, J.E. Bartmess, J.F. Liebman, J.L. Holmes, R.D. Levin, W.G. Mallard, J. Phys. Chem. Ref. Data 17 S1 (1988) 1.
[15] B.P. Tsai, J.H.D. Eland, Int. J. Mass Spectrom. Ion. Proc. 36 (1980) 143.
[16] C.S.S. O'Connor, N.C. Jones, S.D. Price, in preparation.